GEOPERSIA

Accepted Manuscript

Prediction of groundwater level in the southwest plain of Tehran-Iran by Multiple Modelling (MM) and treating heterogeneity by self-organizing map (SOM)

Ali Manafiazar, Mashalah Khamechiyan, Mohammadreza Nikudel, Mohammad Sharifikia

DOI: 10.22059/GEOPE.2024.381089.648773

Receive Date: 20 August 2024
Revise Date: 16 November 2024
Accept Date: 09 December 2024

Prediction of groundwater level in the southwest plain of Tehran-Iran by Multiple Modelling (MM) and treating heterogeneity by self-organizing map (SOM)

Ali Manafiazar [1], Mashalah Khamechiyan [1], *, Mohammadreza Nikudel [1], Mohammad Sharifikiad [2]

[1] Department of Engineering Geology, Faculty of Basic Science, Tarbiat Modares University, Tehran, Iran.
[1] Department of Engineering Geology, Faculty of Basic Science, Tarbiat Modares University, Tehran, Iran.
[1] Department of Engineering Geology, Faculty of Basic Science, Tarbiat Modares University, Tehran, Iran.
[2] Department of Remote Sensing (GIS), Faculty of Humanities, Tarbiat Modares University, Tehran, Iran.

Received: 20 August 2024, Revised: 16 November 2024, Accepted: 09 December 2024

Abstract
Groundwater resources are crucial for meeting water supply needs, highlighting the importance of accurate modeling. The study of groundwater level (GWL) fluctuations holds significant implications for various fields such as management studies, engineering design, agricultural practices, and access to high-quality groundwater. With the increasing use of groundwater resources in recent years, there is a growing need for more serious resource management and closer monitoring of consumption.This research utilized three levels to predict fluctuations in groundwater levels. Firstly, the intelligent self-organizing map (SOM) method was used to cluster observation wells (OWs) in order to reduce heterogeneity in hydrogeological environments. Secondly, models including Sugeno fuzzy logic (SFL), recurrent neural network (RNN), and feedforward neural network (FNN) were utilized to predict groundwater level fluctuations based on regional and observational data, including groundwater level data, groundwater abstraction, temperature, and rainfall. Thirdly, the support vector machine (SVM) Artificial Intelligence (AI) strategy was applied to build further understanding, using the results of the second level as input data to improve results. The findings of this study indicate that the SFL model outperforms the other two models at the second level. Additionally, in the third level, the SVM model improved the results, with testing phase accuracies for categories 1, 2, and 3 improving from 0.92, 0.91, and 0.94 to 0.98, 0.96, and 0.99 respectively.

Keywords: prediction, GWL, SOM, AI models, Tehran plain.

Introduction

In various parts of the world, particularly in arid and semi-arid regions, groundwater serves as one of the most substantial sources for agriculture, drinking, and industrial activities (Barzegar et al., 2017, Neshat et al., 2014). Access to groundwater resources is directly linked to socio-economic development. In recent years, population growth and climate change in developing areas have significantly impacted drinking water consumption patterns, leading to a gradual

* Corresponding author e-mail: khamechm@modares.ac.ir

decline in groundwater quality and scarcity of resources (Huang et al., 2023, Chen et al., 2019, Minnig et al., 2018, Wakode et al., 2018).

Presently, hydrological studies encompass a broad range of activities, including (i) investigating groundwater resources; (ii) determining available groundwater potential; (iii) forecasting changes in GWLs; (iv) exploring aquifer hydraulic conductivity; and (v) planning and managing water resources to enhance aquifer conditions (Razzagh et al., 2021; Nadiri et al., 2021; Mohebbi Tafreshi et al., 2020; Moges et al., 2019; Fijani et al., 2013). Inappropriate exploitation of groundwater resources could result in irreparable damage, such as declining GWLs, deteriorating groundwater quality, and land subsidence (Mahmodpour et al., 2016). Groundwater systems are characterized by nonlinearity, complexity, multi-scale, and random features, all influenced by natural and/or anthropogenic factors, thus complicating dynamic predictions. While mathematical and conceptual models are the primary tools for representing hydrological variables, in numerous cases, they are not suitable; for instance, when precise prediction holds greater importance than physical perception and there is insufficient data, artificial intelligence models can be a viable option for hydrogeological studies (Aryaazar et al., 2021, Nadiri et al., 2014).

Recently, a substantial body of research has focused on the prediction and estimation of hydrological and hydrogeological parameters through the application of artificial intelligence models (Samadi et al., 2023 (a); Samadi et al., 2023 (b); Sharafati et al., 2020; Rajaee et al., 2019; Naganna and Deka., 2019; Manafiazar et al., 2019 a,b). The modeling of aquifers to forecast GWL is crucial for understanding groundwater resources and their effective management in agricultural, industrial, and domestic uses, as well as for the design of engineering structures. Given the mounting concerns regarding groundwater resources and the necessity for accurate forecasts, extensive studies have sought to harness artificial intelligence for predicting GWL. The capacity of the artificial intelligence models to identify patterns enables the resolution of complex hydrological challenges. Noteworthy studies employing artificial intelligence include the evaluation of GWLs fluctuations (Daneshmand et al., 2023; Roshni et al., 2019; Shiri et al., 2013; Hamed et al., 2015; Nourani et al., 2008), estimation of hydraulic conductivity (Sihag., 2018; Nadiri et al., 2014), estimation of vulnerability (Manafiazar et al., 2023; Nadiri et al., 2018; Baghapour et al., 2016) and spatial prediction of hydro-chemical parameters (Benaafi et al., 2022; Kumar Chaudhry et al., 2019).

The inherent ability of individual AI models to predict and estimate hydrogeological parameters results in reduced accuracy and efficiency in heterogeneous study environments. To mitigate the problem of heterogeneity, combining different categories with artificial intelligence models may prove beneficial. Artificial intelligence classification methods hold an advantage over statistical methods requiring significant data and linear mode, as they are compatible with complex multiple aquifer systems and accommodate nonlinear modes. One such classification model is the Self Organizing Map (SOM), which has been increasingly utilized in conjunction with various models of artificial intelligence (Gholami et al., 2020; Haselbeck et al., 2019; Nourani et al., 2016).

The southwestern plain of Tehran is characterized as an arid and semi-arid region of Iran. Over recent years, many reports of subsidence in this plain have become increasingly prevalent due to the excessive use of groundwater resources (Manafiazar et al., 2023; Rajabi Baniani et al., 2021, Mohebbi Tafreshi et al., 2020; Haghshenas Haghighi and Motagh., 2019, Pirouzi and Eslami., 2017, Mahmoudpour et al., 2016). Given that the primary agricultural and industrial water supply of this area depends on groundwater, improper control of groundwater extraction and inadequate resource management are likely to cause irreparable issues (Panahi et al., 2017; Pirouzi and Eslami, 2017).

In this research, we utilized various methods to address the diverse conditions of the area of interest and develop an effective model for predicting and managing groundwater resources.

Specifically, we employed the SOM classification method in level 1. Additionally, in level 2, we utilized feedforward neural network models, recurrent neural networks, and Sugeno fuzzy logic to assess and predict groundwater fluctuations in the southwestern plain of Tehran. Furthermore, the support vector machine was applied in level 3, building upon the results from level 2 as input data.

Materials and Methods

Methodology

In order to predict groundwater levels (GWL), a three-level modeling approach has been developed, as demonstrated in Figure 1. In the first level, the SOM model is utilized to categorize observation wells (OWs) in the plain, aiming to mitigate the heterogeneity of the aquifer environment. Subsequently, at level 2, three artificial intelligence (AI) models are employed to forecast GWL fluctuations. Lastly, at level 3, the SVM model is used to integrate the four models from level 2, in order to explore potential enhancements in their performance.

Self-Organizing Map (SOM)

The main objectives of clustering are data classification, homogeneous data construction, and model structure optimization through the selection of dominant and related inputs. SOM is an artificial intelligence method first developed by Kohonen et al. (1997), characterized by its ability to display a regular distribution of large dimensions on a small, compact system. As a result, SOM can simplify the complex nonlinear relationship in a large dataset into a more manageable display, while also preserving the original data topology structure of the data (Kohonen, 1982). This method offers advantages over other classification methods, such as the lack of an output target function for optimization or prediction (unsupervised learning algorithm) and the categorization of inputs based on similarities without assigned tags (Kohonen, 1982). In this classification, inputs are assigned a random weight between zero and one upon entry into the system. Subsequently, the distance between each input parameter and the center of the hidden layer is determined based on the competition phase and the minimum function.

The SOM training process entails three stages: competition, collaboration, and adaptation. During the competition phase, the data introduced to the network are evaluated to ascertain the minimum distance to the output layer neurons.

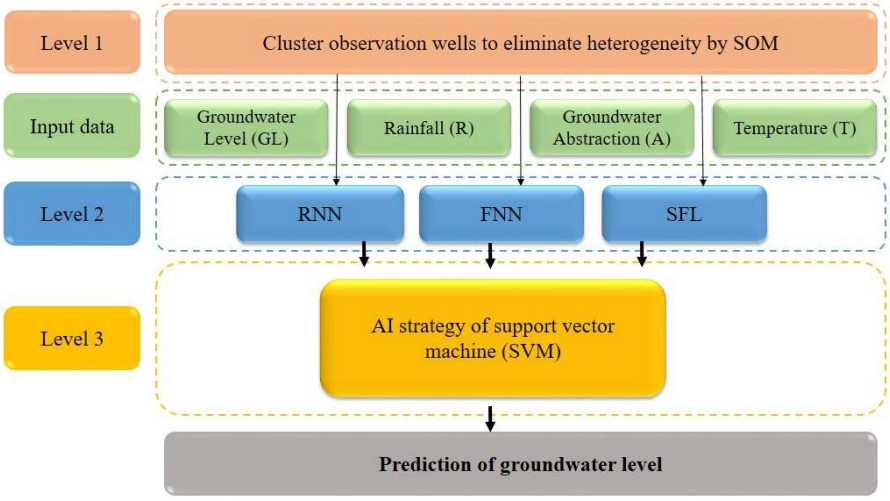

Figure. 1. Flowchart of AI model with multiple levels

The neuron with the least distance was then selected as the winning neuron. The calculation of the Euclidean distance (D_j) in the SOM network is determined according to equation (1) (Kohonen et al., 1997). In this equation, x is the input vector of the winning neurons i, and w_j is the weight of the neighboring neurons.

$$D_j = |x - w_j| \sqrt{\sum_{i=1}^{M} (x_i - w_{ij})^2} \quad (1)$$
$$j = 1,2,3, \dots, M$$

In the collaboration phase, the weights of neighboring neurons are coordinated with the neurons in terms of distance (Kohonen et al., 1997):

$$h_{ij}(x) = (FD_{ij}) \quad (2)$$

In equation (2), the function h_{ij} is created by the effect of the neuron i on the neuron j when the x input is used, indicating that it is formed directly from the distance between neurons i and j (FD_{ij}).

Artificial Neural Network (ANN)

Artificial neural networks are systems used for processing a large amount of information, working in parallel, and modeling the functionality of the human brain's neural network (Hopfield, 1982). The structure of neural networks is based on several key components: (i) nodes that process data; (ii) communication vectors for transferring signals between nodes; (iii) weight assigned to communication lines based on input data importance, and (iv) nodes equipped with activation and conversion functions to produce output signals from network input data. A network usually comprises three layers: input, middle, and output. The input layer serves to input where each node may originate from input variables or output of other nodes, and the middle layer functions as a processor that determines the number of nodes via trial and error. Finally, the output layer contains the predicted values. Artificial neural networks have several notable applications, including pattern segmentation (data and shapes), predictions in various fields, optimization, memory storage, and system control. Multilayer artificial neural networks are comprised of processing nodes (resembling brain neurons) across distinct layers with connections (akin to brain synapses) that link the nodes (Coppola et al., 2003).

Recurrent Neural Network (RNN) is a type of neural network that features connections between nodes over a temporal sequence, forming a directional graph. Time sequence refers to data that is transmitted over time. In this network, information flows between nodes in two directions, from input to output, and this flow can be reversed from output to input. The return network first turns the independent activators into dependent ones. It also assigns the same weight and bias to all layers, which reduces the complexity of RNN parameters. By utilizing the previous output as the input for the subsequent layer, the network provides a standard platform for preserving previous output, enabling data to cycle back into the input (ASCE, 2000).

Feedforward Neural Network (FNN) is characterized by processing nodes located in hidden layers, with networks potentially having multiple hidden layers and a middle layer featuring multiple nodes. Information moves unidirectional, from input to output. Nodes within a layer lack connections, but each node links to the subsequent layer, so anode's output is contingent on the signal it receives from the preceding layer, the assigned weight, and the conversion function type (Coulibaly et al, 2000).

Sugeno Fuzzy logic (SFL)

The Fuzzy Logic (FL) theory, introduced by Zadeh in 1965, is a valuable tool for solving complex

problems across various fields. The theory of fuzzy sets establishes a link between a set of input data and a set of output data. Each FL set employs a Membership Function (MF) with different shapes such as Gaussian, S-shape, sigmoid, triangular, Z-shape, and trapezoidal. The specific form of the MF is determined through trial and error. In classical set theory, an object belongs to a set if its membership value is 1, and it does not belong to the set if its membership value is 0. The Sugeno Fuzzy Logic (SFL) model is built on FL principles. The outputs of SFL are linear functions, utilizing constant or linear output membership functions, referred to as zero-order or first-order SFL, respectively (Sugeno, 1985). Additionally, Soft Computing (SC) is employed to extract fuzzy if-then rules (Chiu, 1994, Chen and Wang, 1999) in the SFL model. Within SC methods, the number of rules corresponds to the number of clusters and is regulated by the clustering radius, which ranges between 0 and 1. The ultimate output of the system is the aggregated weighted average of all rule outputs, computed as follows:

$$GL_{out} = \frac{\sum_i w_i GL}{\sum_i w_i} \quad (4)$$

Where; GL_{out} is the final output of the fuzzy system, w_i is the weight of the ith rule and GL is the output of the ith rule.

Support Vector Machine (SVM)

The support vector machine (SVM) is a machine-learning method that was first introduced by Vapnik in 1995. It is known for applying the inductive principle of structural error minimization, which leads to an overall optimal solution. SVM has been found to produce highly accurate results and is also compatible with sparse data, making it a valuable tool in machine learning (Behzad et al., 2009). The main process in the SVM model involves selecting support vectors and determining their weight. In the context of a dataset with N samples, denoted as (x, y), where x represents the input vectors and y represents the output vectors, the SVM estimator (f(x)) is expressed as equation (3).

$$f(x) = w.\varphi(x) + b \quad (3)$$

Where; w, weight vector; b, bias, and φ are a linear converter function called a Kernel that plots the input vector as a higher space. The objective function of convex optimization using the insensitivity loss function to solve equation (3) is introduced by Vapnik as follows (Vapnik, 1995):

$$minimize\ w'b'\xi'\xi^* = \frac{1}{2}\|w\|^2 + c\sum_{k=1}^{N}(\xi_k + \xi_k^*) \quad (4)$$

$$subject\ to \begin{Bmatrix} y_k - w^T\varphi(X_k) - b \le \varepsilon + \xi_k \\ w^T\varphi(X_k) + b - y_k \le \varepsilon + \xi_k^* \\ \xi_k, \xi_k^* \ge 0 \\ k = 1,2,3,\dots,N \end{Bmatrix}$$

In this equation ξ_k and ξ_k^* are deficient variables that find the training error by the insensitive loss function (ε) and the positive parameter c is the balance coefficient to determine the degree of experimental error in the optimization problem.

In this research, the Kernel of the radial basis function (RBF-Kernel; Radial Basis Function Kernel) and linear kernel (Lin-kernel) were used. The RBF kernel is described in Equation (5), where the parameter σ is related to the kernel function.

$$(X_k, X_1) = \exp\left(-\frac{\|X_k - X_1\|^2}{2\sigma^2}\right) \quad (5)$$

To address the computational cost associated with solving large-scale problems using the

SVM model, Suykens et al., (2002) proposed the Least Squares Support Vector Machine (LSSVM) method.

Study area

Tehran plain has a slope from north to south, which is located in the 50° 55′ E to 51° 23′ E and 35° 30′ N to 35° 42′ N. The area of the Tehran plain is more than 2250km^2, of which about 350km^2, is the foothills and protrusions inside the plain, and 1900 square kilometers is the flat part of the plain. The study area is approximately 415 km^2 (Figure.2). The average height of the plain is 1100 meters. The maximum and minimum height of the studied plain are shown in Figure.3. In general, ten rivers enter the Tehran plain, the most important rivers charging the Tehran plain are the Karaj and Kan rivers (Mahmoudpour et al., 2016).

Geology context

The topography of the Tehran basin is generally characterized by a flat landscape with a gradual decline in elevation. Covering an area of 2250 km2, the alluvial groundwater of the basin is typical of a variety of soil particle sizes, forming lenses of varying thicknesses. The alluvial deposits in the Tehran Plain are categorized into four geological structures (Rieben, 1955) (Figure.2):

A) Hezardarreh formation: This formation displays regular stratification and consists of conglomerates with lenses of sandstone and mudstone, with an approximate thickness of 1200 m.

B) Qt1 of the Kahrizak formation: Comprising sandy silt, the reach of this deposit in the southern region of the Tehran basin is not definitively known.

C) Qt2 of Tehran alluvial formation: This unit is predominantly found in the southern portion of the plain. The northern part of the unit is predominantly made up of irregularly laminated gravel, with silty deposits increasing in size towards the south. The maximum thickness of Tehran's alluvial deposit is approximately 60 m.

D) Recent alluvia: This unit includes pebbly and fine silt in specific locations, with fine grains such as clay and silt predominating in the southern plain.

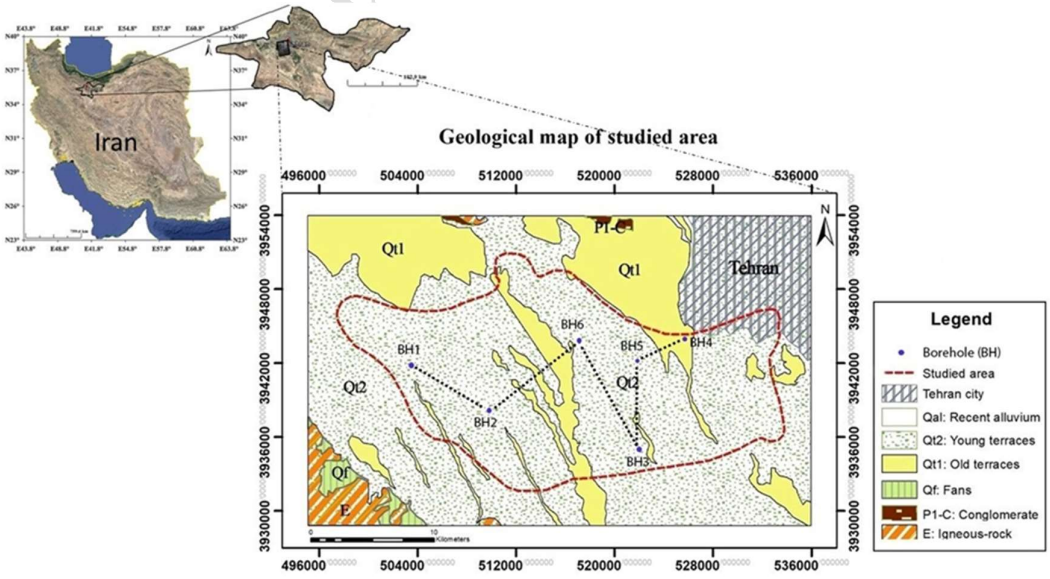

Figure 2. The geography and geology chart of the Tehran plain

Hydrogeology of the study area

The alluvial plain located to the southwest of Tehran exhibits various subsurface complexities. Changes in the permeability and depth of the bedrock, local hydrogeological features, and geometric features of groundwater passages, aquifer recharge, and lateral drainage, have caused deviations in the general direction of groundwater flow within certain areas of the plain. The aquifer units primarily consist of fine-grained clay units typified by low permeability, such as silty clays and clay silt (Figure 4).

The thickness of the alluvial aquifer in the Tehran region is estimated to be between 300 and 350 meters, consisting of the second member of the Hezardarreh formation along with younger formations. Generally, the Tehran Alluvial formation is made up of heterogeneous grains and is permeable due to the weak cement binding the pebbles, while also exhibiting relatively high mechanical resistance. The Tehran Alluvial deposits provide better underground water within the alluvial fan of the region. The primary alluvial fans in Tehran, listed from west to east, are Karaj, Kan, and Jajrud. The recent alluvium from the Holocene epoch comprises distinct and highly permeable deposits, with varying mechanical resistance across different areas of the region.

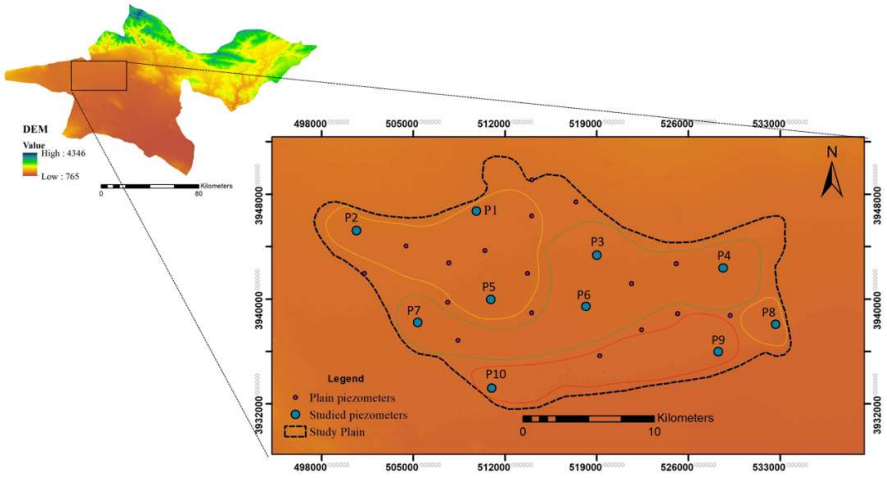

Figure 3. Location of piezometers in the plain southwest of Tehran

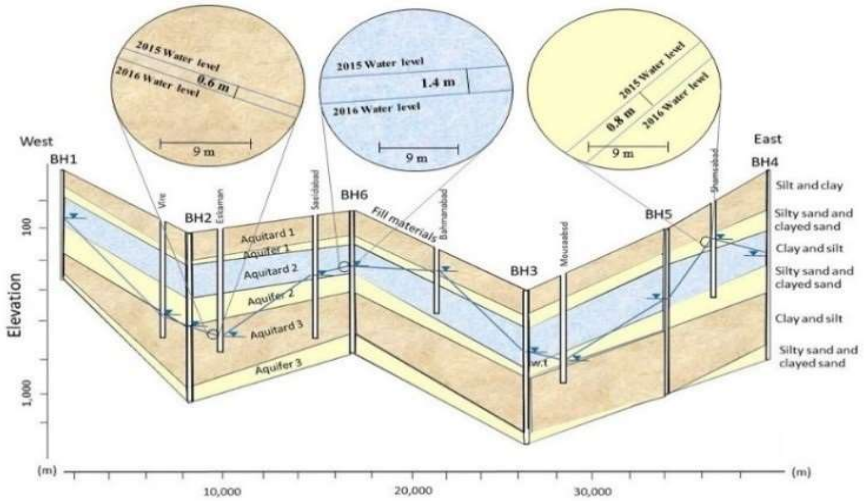

Figure 4. Hydrogeological cross-section that illustrates the research region layers of the aquifer system (Manafiazar et al., 2023)

Conversely, in some northern, eastern, and southwestern segments, the bedrock elevation contributes to an alluvium thickness of less than 25 meters. As depicted in Figure 4, the study area contains 27 piezometer wells for observation purposes. The study and modeling of groundwater within this plain hold great significance in managing regional water resources, particularly in the context of agriculture, uncontrolled abstraction of groundwater resources, and the adverse effects of water level depletion, including severe land subsidence (Manafiazar et al., 2023).

Data analysis

Model input data

The selection of input variables in artificial intelligence models is a critical consideration for achieving accurate outputs. In the plain southwest of Tehran, there are 27 OWs, of 10 of these piezometers with 5 years of GWL data (2017-2022) have been utilized for modeling and forecasting the aquifer GWL, as illustrated in Figure 3. Additionally, Table 2 presents the geographical location and GWL statistics for the studied piezometers in the southwestern plain of Tehran. In this study, average monthly GWL, average monthly rainfall, average monthly temperature, and monthly groundwater abstraction at each time step t_0 and from GWL in time step t_{0-1} due to the effect of these two components on GWL in the period 2015-2022 as input and also, GWL at time t_0 was used as the output of artificial intelligence models including RNN, FNN, and SFL. Thus 80 percent of the available data was allocated as normal input data for the training of the models, while the remaining 20 percent of the data was utilized for testing.

The average annual rainfall in the southern Tehran plain is recorded at less than 200 mm, while the northern region receives about 500 mm. Statistical data on rainfall in the region indicates an increasing trend from the south to the north, with an estimated average of 250 mm. The rainfall pattern is characteristic of a Mediterranean climate. Figure. (5a) illustrates the annual variations in rainfall in the southwestern Tehran plain from 2017 to 2022.

In terms of temperature, the average daily temperature ranges from 10 °C in mountainous areas to a maximum of 42 °C, with a recorded minimum of -10.5 °C. The coldest and warmest months in the region are January and August, respectively. The temperature fluctuations over the period 2017 to 2022 are depicted in Figure. (5b).

Based on the report from Tehran Regional Water Company (TRWC) in 2022, the number of groundwater extraction wells in the study area increased from 31568 in 2017 to 35393 in 2022. Additionally, the annual groundwater abstraction also rose from 865.32 million m^3 to 1123.51 million m^3. Figure. 5c depicts the yearly changes in groundwater abstraction in the southwestern Tehran plain from 2017 to 2022, while Figure. 6 displays the locations of withdrawal wells in the study plain. Table 3 shows the average value of determined data of rainfall, temperature, and groundwater abstraction from 2017 to 2022.

Table 2. A summary of statistics of piezometers studied in the southwestern plain of Tehran

The name of the piezometer	Baba salman (P1)	Kordzar (P2)	Ahmad abad (P3)	Benz Khavar (P4)	Eskaman (P5)	Bahman abad (P6)	Yousef abad (P7)	Placin (P8)	Jafarabad (P9)	Aderan (P10)
Geographical location	X:510975 Y:3933203	X:500663 Y:3945240	X:518996 Y:3943371	X:528636 Y:3942382	X:510900 Y:3939980	X:518151 Y:3939443	X:492025 Y:3948063	X:532659 Y:3938087	X:528264 Y:3936008	X:510975 Y:3933203
Average GWL (m)	1044.8	1043.7	1065.38	1071.22	1054.75	1053.55	1075.41	1046.93	1031.15	1014.11

Table 3. The average value of determined data of rainfall, temperature, and groundwater abstraction from 2017 to 2022

Average rainfall for 5 years (mm)	Average temperature for 5 years (°C)	Average groundwater abstraction for 5 years (million m^3)
33.60	18.55	997.80

Figure 5. Graph of annual (a) rainfall (b) temperature, and (c) groundwater abstraction fluctuations in Tehran Plain from 2017 to 2022

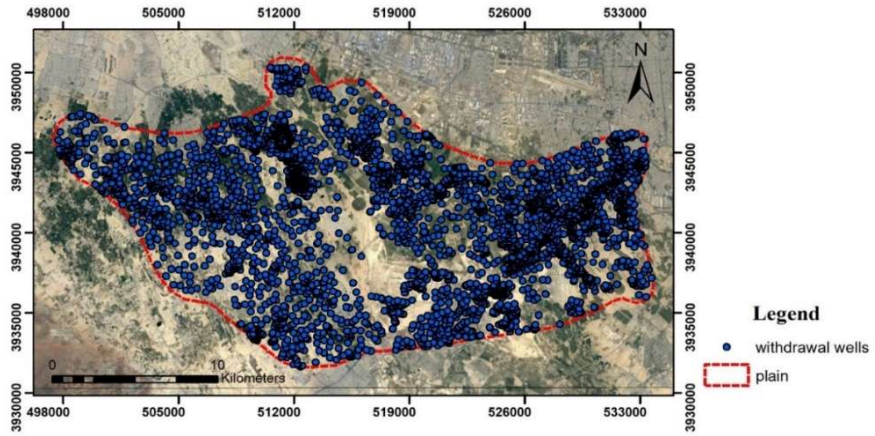

Figure 6. Location of withdrawal wells in the study plain

Model evaluation criteria

In this research, to evaluate the efficiency and capability of the proposed hybrid models, two criteria of Coefficient of determination (R^2), the Root mean squared error (RMSE), were utilized, which are defined as the following equations:

$$R^2 = \frac{\sum_{i=1}^{n}(x_i - \hat{x_i})^2}{\sum_{i=1}^{n}(x_i - x)^2} \quad (6)$$

$$RMSE = \sqrt{\frac{\sum_{i=1}^{n}(x_i - \hat{x_i})^2}{n}} \quad (7)$$

Where: x_i and $\hat{x_i}$, observational and computational values, respectively; x is the mean of the observational values and n is the total number of data. The best values for the mentioned criteria are one and zero, respectively.

Results

The purpose of this study was to examine the differences in groundwater levels in the southwestern plain of Tehran using artificial intelligence models. However, the complex and uneven characteristics of the aquifer system in the area, along with significant variations in water level changes among piezometers, make it challenging to accurately predict groundwater levels using individual models. In order to overcome this issue, piezometer classification methods were used to improve the accuracy of the model and account for the heterogeneous nature of the study area. The SOM intelligent classification method was found to produce more accurate results compared to other classification methods, as indicated in section 2-1 of the research.

Level 1: classification of the study area with SOM

To apply the classification model, 10 piezometers were chosen as inputs, with long-term groundwater level (GWL) data spanning 5 years (2017-2022). The resulting self-organizing map (SOM) model categorized the piezometers into 3 groups, with 4 piezometers in 2 categories and 2 piezometers in the third category. Specific piezometers were allocated to each category, as shown in Figure. 7. The fluctuation in GWL for the piezometers in the first category was illustrated in Figure. 8, demonstrating the model's accurate output.

To predict GWL fluctuations using AI models at level 2, we select one OW from each category of SOM classification. P1 was selected from the first category, P4 from the second category, and P10 from the third category.

Level 2: predicting fluctuations using FNN, RNN, SFL

To implement the feedforward neural network (FNN), recurrent neural network (RNN), and seasonal autoregressive integrated moving average with exogenous variables (SFL) models for each category, all input data were normalized as detailed in section 4-1. The Levenberg-Marquardt Algorithm (LMA) was utilized for FNN and RNN models to predict GWL fluctuations.

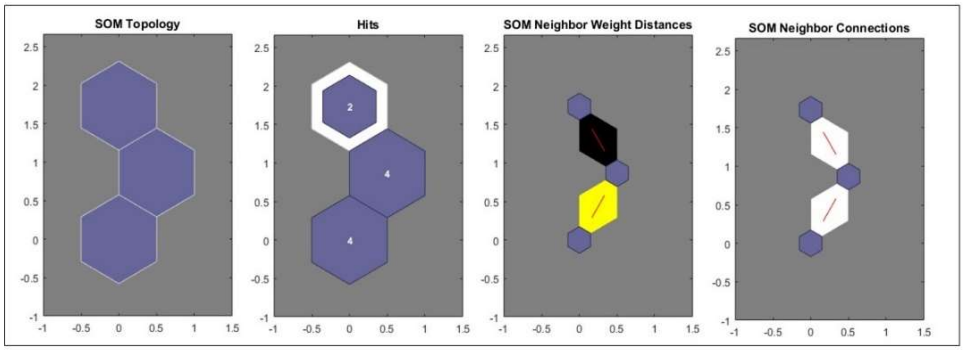

Figure 7. Excitability and final state of neighboring neurons in the SOM model

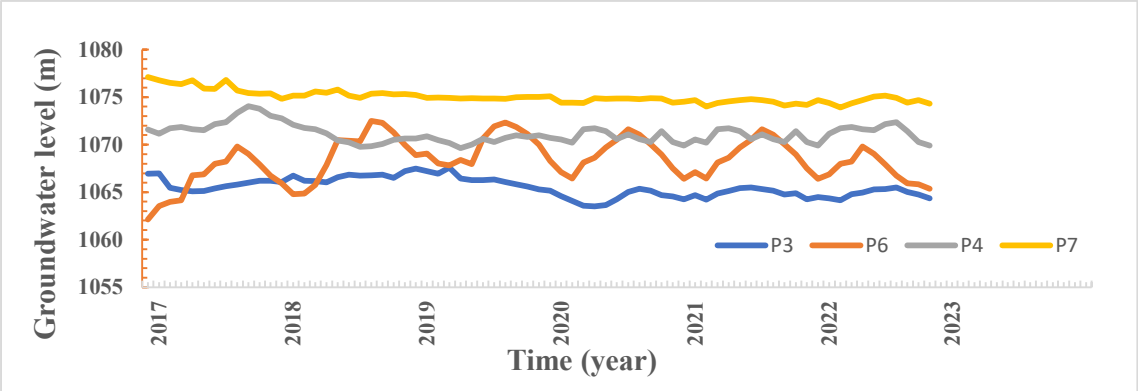

Figure 8. GWL trend in the first category

A normalization process was carried out for all data, followed by a trial and error approach to determine the optimal number of middle layer nodes to maintain the network's elliptical state. One piezometer from each category was chosen for prediction, with 4 inputs including precipitation, temperature, evaporation, and piezometer GWL assigned with a time delay. Table 4 presents the results of individual base models at level 2 for the training and testing stages of FNN and RNN models. The selected piezometer structure for each category in the FNN and RNN models is 4-3-1, with an epoch of 500. SFL is used to establish a base model at Level 2. The method is implemented through the following steps: (i) data classification and identification of Membership Functions (MF) using a Subtractive Clustering (SC) method, (ii) determination of the clustering radius, which ranges from zero to one and governs the number of clusters and if-then rules, as described in Eq. (8) for the GWL, Rainfall, Abstraction, and Temperature variables.

$$Rule\ i\ if \begin{Bmatrix} \left(GWL_{t-1}\ belongs\ MF^{i}_{GL_{t-1}}\right)\ and \\ \left(R\ belons\ to\ MF^{i}_{R}\right)\ and \\ \left(A\ belons\ to\ MF^{i}_{A}\right)\ and \\ \left(T\ belons\ to\ MF^{i}_{T}\right) \end{Bmatrix} then\ \widehat{GL} \quad (8)$$

$$=m_i T + n_i P + p_i Q + qGl_{t-1} + c_i$$

Where GWL_{t-1} is MF of the i^{th}cluster of input GWL; MF^{i}_{R} is MF of the i^{th} cluster of input R; MF^{i}_{A} is MF of the i^{th} cluster of input A; and MF^{i}_{T} is MF of the i^{th}cluster of input A; m_i, n_i, p_i,…, c_i are coefficients of output MF. The MF used for the fuzzy modeling of GWL is a Gaussian function, and the output function of the model is a linear type based on the input data. The weighted average of all the rules is the final output of the model. The RC of each of the first, second, and third categories is 0.7, 0.5, and 0.9, respectively, and the cognitive radio network (CRN) of the first, second, and third categories is 3, 4, and 4, respectively. Table 4 presents the results of individual base models at level 2 for the training and testing phase of the SFL model.

Level 3: SVM model to combine base models at level 2

The Support Vector Machine (SVM) model was applied to combine the base models at Level 2. According to Figure. 1, the GEP model inputs are the outputs of the Level 2 models, and the SVM model targets the GWLt. This study utilized the Radial Basis Function (RBF) for the kernel function, with two parameters (σ and γ) determined through trial and error. The σ for the first, second, and third categories were found to be 12.87, 11.44, and 9.3, respectively, and the

γ for these categories were 440, 386, and 394, respectively. The results of the training and testing phase of the SVM model at level 3 are presented in Table 4.

Table 4 displays the outcomes of the individual basic models at Level 2 and the MM at Level 3 during both the training and testing phases. While the results of the training phase at Level 2 are substantial in terms of [metric], the figures noticeably decline during the testing phases. It is typical for R2 to decrease from the training to testing phases, but the testing phase results serve as the primary basis for evaluation. Although all test outcomes are suitable and justifiable for Level 2, further enhancements could be achieved through combined models, thus necessitating additional research at Level 3. The results from Table 4 indicate that the SVM model has the potential to significantly improve GWL prediction.

The model rankings at Level 2 favor the selection of SFL based on RMSE, and [metric]. The scatter diagram for the base models at both Level 2 and Level 3 (Figure 9, 10, and 11) demonstrates their suitability for their intended purpose. Nevertheless, the scatter diagrams in Figure 9, 10, and 11 depict error residuals (observed - modeled values), revealing that there is little distinction among the base models. This indicates that the FNN, RNN, and SFL models at Level 2 may encounter deviations within the range of ±0.5.

Table 4. Performance measures of different applied models

Level	Model	Category 1 (P1)				Category 2 (P4)				Category 3 (P10)			
		train		test		train		test		train		test	
		R^2	RMSE	R^2	RMSE	R^2	RMSE	R^2	RMSE	R^2	RMSE	R^2	RMSE
2	FNN	0.89	0.17	0.83	0.19	0.92	0.23	0.92	0.21	0.90	0.19	0.89	0.20
	RNN	0.92	0.20	0.91	0.21	0.91	0.19	0.90	0.18	0.89	0.23	0.89	0.19
	SFL	0.94	0.19	0.92	0.16	0.94	0.19	0.91	0.18	0.96	0.18	0.94	0.18
3	SVM	0.96	0.15	0.98	0.12	0.96	0.17	0.96	0.12	0.97	0.13	0.99	0.11

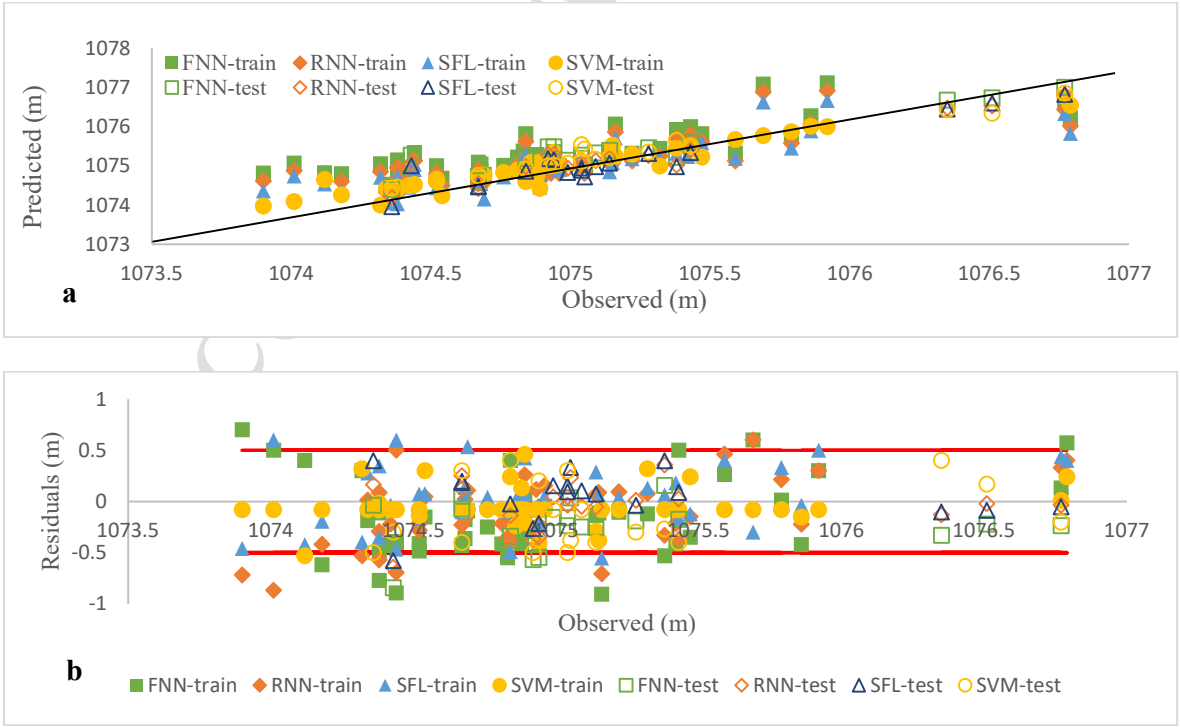

Figure 9. a) Scatter diagram of observed and calculated GWL, b) Residual plot cross GWLs for P1 (Red line is baseline; Y = 0.5 and − 0.5)

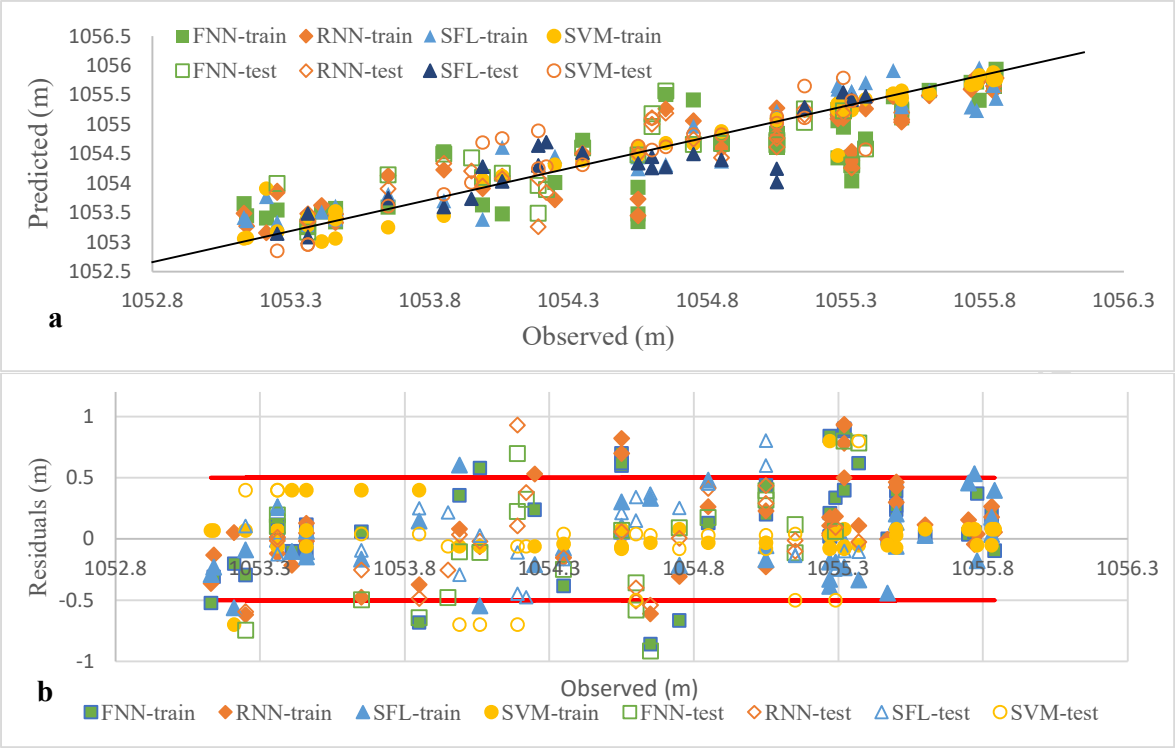

Figure 10. a) Scatter diagram of observed and calculated GWL, b) Residual plot cross GWLs for P4 (Red line is baseline; Y = 0.5 and − 0.5)

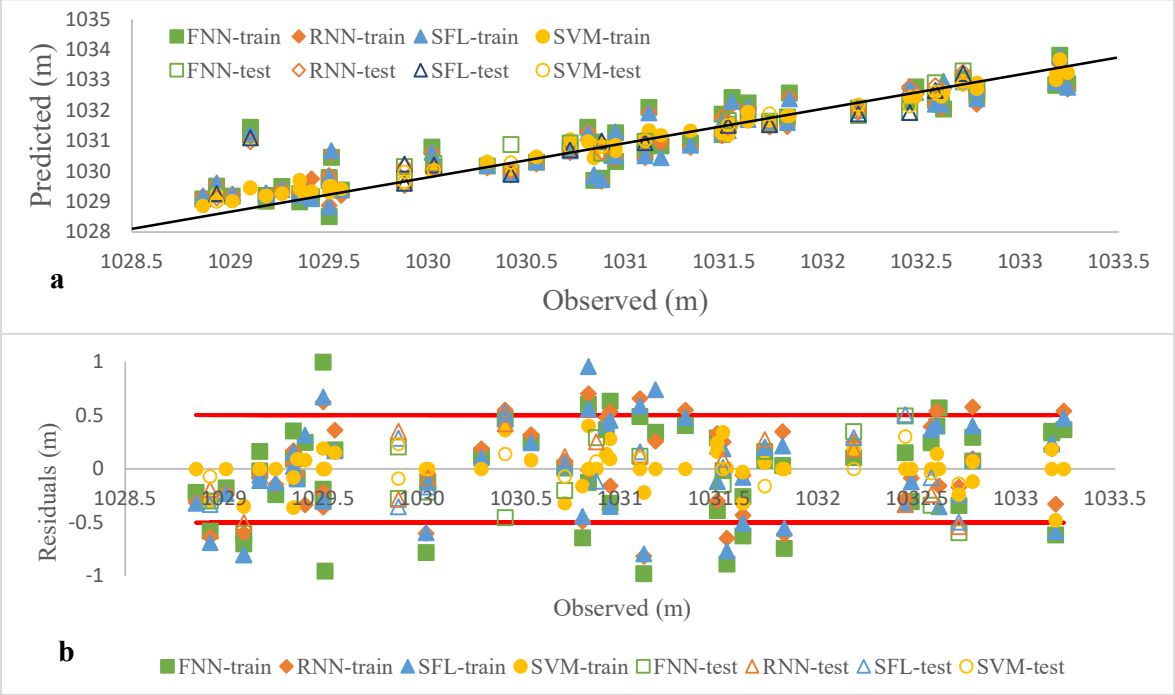

Figure 11. a) Scatter diagram of observed and calculated GWL, b) Residual plot cross GWLs for P10 (Red line is baseline; Y = 0.5 and − 0.5)

Conclusion

This study aims to develop reliable predictions of Groundwater Level (GWL) using a limited

amount of data related to GWL, rainfall, groundwater abstraction, and temperature. The research employs Multiple Modelling (IMM) strategies across three levels to achieve this objective. Firstly, the intelligent self-organizing map (SOM) method is used to cluster observation wells (OWs). Secondly, models such as Sugeno fuzzy logic (SFL), recurrent neural network (RNN), and Feedforward neural network (FNN) are utilized to forecast groundwater level fluctuations. Lastly, the support vector machine (SVM) AI strategy is applied to further enhance understanding, with results from Level 2 reused as input data at Level 3.

Given the abundance of OWs in the region, the SOM model is utilized to cluster the wells and select one from each cluster for investigation. The modeling results indicate that individual models at Level 2 are suitable for their intended purpose, but the IMM strategies at Level 3 improve overall performance. Although this improvement is not evident from performance metrics alone, it is evident when examining scatter diagrams of the error residuals.

The study highlights a significant decrease in groundwater levels in the southwest of Tehran, attributed to the region's large area (415 km2), declining rainfall, and increased utilization of groundwater for agricultural and industrial activities. If left unaddressed, this decline could lead to various problems, including the drying up of water wells, depletion of rivers in the area, and groundwater pollution.

Acknowledgments

This research is financially supported by the Tarbiat Modares University through a Grant scheme.

References

Arya Azar, N., Ghordoyee Milan, S., Kayhomayoon, Z., 2021. the prediction of longitudinal dispersion coefficient in natural streams using LS-SVM and ANFIS optimized by Harris hawk optimization algorithm. Journal of Contaminant Hydrology, 240, 103781. https://doi.org/10.1016/j.jconhyd .2021.103781.

ASCE, Task Committee on Application of Artificial Neural Networks in Hydrology., 2000. Artificial neural network in hydrology, part I and II Journal of Hydrologic Engineering, 5 (2): 115-137.

ASF DAAC, https://search.asf.alaska.edu/.

Baghapour, MA., Nobandegani, AF., Talebbeydokhti, N., Bagherzadeh, S., Nadiri, AA., Gharekhani, M., Chitsazan, N., 2016. Optimization of DRASTIC method by artificial neural network, nitrate vulnerability index, and composite DRASTIC models to assess groundwater vulnerability for unconfined aquifer of Shiraz Plain, Iran. Journal of Environmental Health Science and Engineering 14 (1): 13. https://doi.org/10.1186/s40201-016-0254-y.

Barzegar, R., Fijani, E., Asghari Moghaddam, A., Tziritis, E., 2017. Forecasting of groundwater level fluctuations using ensemble hybrid multi-wavelet neural network-based models. Science of the Total Environment, 599: 20-31.

Behzad, M, Asghar, K., Eazi, M., Palhang, M., 2009. Generalization performance of support vector machines and neural networks in runoff modeling. Expert Systems with Applications, 36 (4): 7624-7629. https://doi.org/10.1016/j.eswa.2008.09.053.

Benaafi, M., Yassin, MA., Usman, AG., Abba, SI., 2022. Neurocomputing Modelling of Hydrochemical and Physical Properties of Groundwater Coupled with Spatial Clustering. GIS, and Statistical Techniques. Sustainability, 14, 2250. https://doi.org/10.3390/su14042250.

Buckley, S., 2000. Radar interferometry measurement of land subsidence Ph.D. dissertation. TX: The University of Texas at Austin. http://dx.doi.org/10.26153/tsw/11126.

Chen, B., Deng, K., Fan, H., Hao, M., 2013. Large-scale deformation monitoring in mining area by D-InSAR and 3D laser scanning technology integration. International Journal of Mining Science and Technology, 23 (4): 555-61. https://doi.org/10.1016/j.ijmst.2013.07.014.

Chen, J., 2019. Satellite gravimetry and mass transport in the Earth system. Geodesy and Geodynamics. 10: 402-415.

Coppola, E., Szidarovszky, F., Poulton, M., Charles, E., 2003. Artificial Neural Network Approach for Predicting Transient Water Levels in a Multilayered Groundwater System under Variable State, Pumping, and Climate Conditions. Journal of Hydrologic Engineering, 6: 348- 360.

Coulibaly, P., Anctil, F., Bobée, B., 2000. Daily reservoir inflow forecasting using artificial neural networks with a stopped training approach. Journal of Hydrology, 230: 244-257.

Daneshmand, F., Adamowski, J., Martel, R., 2023. Regional Groundwater Flow Modeling Using Improved Isogeometric Analysis: Application and Implications in Unconfined Aquifer Systems. Water Resources Management. https://doi.org/10.1007/s11269-023-03631-9.

Fijani, E., Nadiri, AA., Moghaddam, AA., Tasi, FT., Dixon, B., 2013. Optimization of DRASTIC method by supervised committee machine artificial intelligence to assess groundwater vulnerability for Maragheh-Bonab plain aquifer, Iran. Journal of Hydrology, 503: 89-100.

Galloway, D., Burbey, T., 2011. Review: regional land subsidence accompanying groundwater extraction, Hydrogeology Journal, 19, 1459- 1486. https://doi.org/10.1007/s10040-011-0775-5.

Gholami, V., Khaleghi, MR., Taghvaye Salimi, E., 2020. Groundwater quality modeling using self-organizing map (SOM) and geographic information system (GIS) on the Caspian southern coasts. J. Mt. Sci. 17, 1724-1734. https://doi.org/10.1007/s11629-019-5483-y.

Haghshenas Haghighi, M., Motagh, M., 2019. Ground surface response to continuous compaction of aquifer system in Tehran, Iran: Results from a long-term multi-sensor InSAR analysis. Remote Sensing of Environment. 221, 534-550. https://doi.org/10.1016/j.rse.2018.11.003.

Hamed, Y., Elkiki, M., Gahtani, OS., 2015. Prediction of future groundwater level using artificial neural network, Southern Riyadh, KSA (case study). International Water Technology Journal, 5(2): 149-169.

Haselbeck, V., Koedilla, J., Krause, F., Sauter, M., 2019. Self-organizing maps for the identification of groundwater salinity sources based on hydrochemical data. Journal of Hydrology, 576, 610-619. https://doi.org/10.1016/j.jhydrol.2019.06.053.

Hopfield, J. J., 1982. Neural network and physical ayatems with emergent collective computational abilities Proceeding of the national academy of sciences of the United States of America, 79: 2554-2558.

Huang, Zh., Yuan, X., Sun, S., Leng, G., Tang, Q., 2023. Groundwater Depletion Rate Over China During 1965-2016: The Long-Term Trend and Inter-annual Variation. JGR Atmospheres, 128: 11. https://doi.org/10.1029/2022JD038109.

Kohonen, T., Kaski, S., Lappalainen, H., 1997. Self-organized formation of various invariant-feature filters in the adaptive subspace SOM. Neural Computation. 9(6): 1321-1344.

Kohonen, T., 1982. Self-organized formation of topologically correct feature maps. Biological cybernetics. 43(1): 59-69.

Kumar Chaudhry, A., Kumar, K., Afaq Alam, M., 2019. Spatial distribution of physico-chemical parameters for groundwater quality evaluation in a part of Satluj River Basin, India. Water Supply; 19 (5): 1480-1490.

Luo, Q., Perissin, D., Zhang, Y., Jia, YL., 2014. X-Band Multi-Temporal InSAR Analysis of Tianjin Subsidence. Remote Sens, 6: 7933-7951.

Mahmodpour, M., Khamechian, M., Nikudel, MR., 2016. Numerical simulation and prediction of regional land subsidence caused by groundwater exploitation in the southwest plain of Tehran, Iran. Engineering Geology 201, 6-28. https://doi.org/10.1016/j.enggeo.2015.12.004.

Massonnet, D., Feigl, K., 1998. Radar interferometry and its application to changes in the Earth's surface. Rev Geophys, 36 (4): 441-500.

Manafiazar, A., Khamehchiyan, M., Nadiri, AA., and Sharifikia, M., 2023. Learning simple additive weighting parameters for subsidence vulnerability indices in Tehran plain (Iran) by artificial intelligence methods. European Journal of Environmental and Civil Engineering, 28 (1): 108-127 .

Manafiazar, A., Khamehchiyan, M., Nadiri, A.,2019a. Comparison of Vulnerability of the Southwest Tehran Plain Aquifer with Simple Weighting Model (ALPRIFT Model) and Genetic Algorithm (GA). KJES , 4 (2) :199-212 URL: http://gnf.khu.ac.ir/article-1-2665-fa.html [In Persian].

Manafiazar, A., Khamehchiyan, M., Nadiri, A.,2019b. Optimization of the ALPRIFT method using a support vector machine (SVM) to assess the subsidence Vulnerability of the southwestern plain of Tehran. Scientific quarterly journal of Iranian association of engineering geology, 11 (2), 1-14. URL: https://www.jiraeg.ir/article_83263_en.html [In Persian].

Minnig, M., Moeck, C., Radny, D., Schirmer, M., 2018. Impact of urbanization on groundwater recharge rates in Dübendorf. Switzerland. Journal of Hydrology, 563: 1135-1146.
Moges, DM., Bhat, HG., Thrivikramji, KP., 2019. Investigation of groundwater resources in highland Ethiopia using a geospatial technology. Model. Earth Syst. Environ. 5: 1333-1345.
Mohebbi Tafreshi, G., Nakhaei, M., Lak, RA., 2020. GIS-based comparative study of hybrid fuzzy-gene expression programming and hybrid fuzzy-artificial neural network for land subsidence susceptibility modeling. Stochastic Environmental Research and Risk Assessment, 34: 1059-1087.
Mohebbi Tafreshi, G., Nakhaei, M., Lak, R., 2021. Land subsidence risk assessment using GIS fuzzy logic spatial modeling in Varamin aquifer, Iran. GeoJournal, 86: 1203-1223.
Nadiri, AA., Chitsazan, N., Frank, TC., Tsai, M., and Asghari Moghaddam, A., 2014. Bayesian Artificial Intelligence Model Averaging for Hydraulic Conductivity Estimation. Journal of Hydrologic Engineering, 19: 520- 532.
Nadiri, AA., Sadeghfam, S., Gharekhani, M., Khatibi, R., and Akbari, E., 2018. Introducing the risk aggregation problem to aquifers exposed to impacts of anthropogenic and geogenic origins on a modular basis using 'risk cell'. Journal of Environmental Management, 217: 654-667.
Nadiri, AA., Razzagh, S., Khatibi, R. et al 2021. Predictive groundwater levels modelling by Inclusive Multiple Modelling (IMM) at multiple levels. Earth Sci Inform, 14: 749-763.
Naganna, SR., Deka, PC., 2019. Artificial intelligence approaches for spatial modeling of streambed hydraulic conductivity. Acta Geophysica, 67: 891-903.
Neshat, A., Pradhan, B., Dadras, M., 2014. Groundwater vulnerability assessment using an improved DRASTIC method in GIS. Resources, Conservation and Recycling. 86: 74-86.
Nourani, V., Asgharimoghaddam, AA., Nadiri, A., Singh, VP., 2008. Forecasting spatiotemporal water levels of Tabriz aquifer. Trends in Applied Sciences Research 3 (4): 319- 329.
Nourani, V., Taghi Alami, M., Daneshvar Vousoughi, F., 2016. Hybrid of SOM-Clustering Method and Wavelet-ANFIS Approach to Model and Infll Missing Groundwater Level Data. Journal of Hydrologic Engineering, 21(9): 05016018. https://doi.org/10.1061/(ASCE)HE.1943-5584.0001398.
Panahi, MR., Mousavi, SM., Rahimzadegan, M., 2017. Delineation of groundwater potential zones using remote sensing, GIS, and AHP technique in Tehran-Karaj plain, Iran. Environmental Earth Sciences, 76: 792. https://doi.org/10.1007/s12665-017-7126-3.
Pirouzi, A., Eslami, A., 2017. Ground subsidence in plains around Tehran: site survey, records compilation and analysis. International Journal of Geo-Engineering, 8:30. https://doi.org/10.1186/s40703-017-0069-4.
Pisner, DA., Schnyer, DM., 2020. Chapter 6 - Support vector machine, Machine Learning, Academic Press, 101-121. https://doi.org/10.1016/B978-0-12-815739-8.00006-7.
Rajabi Baniani, S., Chang, L., Maghsoudi, Y., 2021. Mapping and analyzing land subsidence for Tehran using Sentinel-1 SAR and GPS and geological data. EGU General Assembly. https://doi.org/10.5194/egusphere-egu21-295.
Rajaee, T., Ebrahimi, H., Nourani, V., 2019. A review of the artificial intelligence methods in groundwater level modeling. Journal of Hydrology, 572: 336-351.
Razzagh, S., Sadeghfam, S., Nadiri, AA., 2022. Formulation of Shannon entropy model averaging for groundwater level prediction using artificial intelligence models. International Journal of Environmental Science and Technology. 19: 6203-6220.
Rosen, P., 2014. UNAVCO short course: Principles and theory of radar interferometry. Presented at InSAR: An introduction to processing and applications using ISCE and GIAnT, Boulder, CO, 4-6.
Rieben, EH., 1955. the geology of the Tehran plain. American Journal of Science 253: 617-639.
Roshni, T., Jha, MK., Deo, RC., Vandana, A., 2019. Development and Evaluation of Hybrid Artificial Neural Network Architectures for Modeling Spatio-Temporal Groundwater Fluctuations in a Complex Aquifer System. Water Resources Management, 33: 2381-2397.
Sarscape, 2014. https://www.sarmap.ch/index.php/software/sarscape.
Samadi, H., Mahmoodzadeh, A., Hussein Mohammed, A et al 2023. Application of Several Fuzzy-Based Techniques for Estimating Tunnel Boring Machine Performance in Metamorphic Rocks. Rock Mechanics and Rock Engineering. https://doi.org/10.1007/s00603-023-03602-x.
Samadi, H., Hassanpour, J., Rostami, J., 2023. Prediction of Earth Pressure Balance for EPB-TBM Using Machine Learning Algorithms. International Journal of Geo-Engineering ,14 (11). https://doi.org/10.1186/s40703-023-00198-7.

Sharafati, A., Asadollah, SBHS., Neshatd, A., 2020. A new artificial intelligence strategy for predicting the groundwater level over the Rafsanjan aquifer in Iran. Journal of Hydrology, 591: 125468. https://doi.org/10.1016/j.jhydrol.2020.125468.

Shiri, J., Kisib, O., Yoon, H., Lee, KK., Nazemia, AH., 2013. Predicting groundwater level fluctuations with meteorological effect implications A comparative study among soft computing techniques. Computers & Geosciences, 56: 32-44.

Sihag, P., 2018. Prediction of unsaturated hydraulic conductivity using fuzzy logic and artificial neural network. Modeling Earth Systems and Environment, 4:189-198. https://doi.org/10.1007/s40808-018-0434-0.

Simmons, BS., Wempen, JM., 2021. Quantifying relationships between subsidence and longwall face advance using DInSAR. International Journal of Mining Science and Technology, 31(1): 91-94.

Suykens, JA., De Brabanter, J., Lukas, L., Vandewalle, J., 2002. Weighted least squares support vector machines: robustness and spare approximation. Neurocomputing. 48(1): 85-105.

Tomás, R., Romero, R., Mulas, J., Marturià, JJ., Mallorquí, JJ., Lopez-Sanchez, JM., Herrera, G., Gutiérrez, F., González, PJ., Fernández, J., Duque, S., Concha-Dimas, A., Cocksley, G., Castañeda, C., Carrasco, D., Blanco, P., 2014. Radar interferometry techniques for the study of ground subsidence phenomena: a review of practical issues through cases in Spain, Environmental Earth Sciences , 71: 163-181.

Vapnik, VN., 1995. the nature of statistical learning theory. Springer. New York. 150 p. ISBN 978-1-4757-3264-1. https://doi.org/10.1007/978-1-4757-3264-1.

Vervoort, A., Declercq, P., 2018. Upward surface movement above deep coal mines after closure and flooding of underground workings. International Journal of Mining Science and Technology; 28: 9-53.

Wakode, HB., Baier, K., Jha, R., Azzam, R., 2018. Impact of urbanization on groundwater recharge and urban water balance for the city of Hyderabad. Indihttps://doi.org/10.1016/j.iswcr.2017.10.003.

Wempen, J., 2020. Application of DInSAR for short period monitoring of initial subsidence due to longwall mining in the mountain west United States. International Journal of Mining Science and Technology, 30 (1): 23-25.

Zhang, Y., 2012. Support Vector Machine Classification Algorithm and Its Application. In: Liu, C., Wang, L., Yang, A. (eds) Information Computing and Applications. ICICA 2012. Communications in Computer and Information Science, vol 308. Springer, Berlin, Heidelberg. https://doi.org/10.1007/978-3-642-34041-3_27.